Geoscience Frontiers 11 (2020) 1123–1131

HOSTED BY

Contents lists available at ScienceDirect

Geoscience Frontiers

journal homepage: www.elsevier.com/locate/gsf

Research Paper

Early Cretaceous subduction initiation beneath southern Tibet caused the northward flight of India

Haoyu Hu, Robert J. Stern *

Geosciences Department, University of Texas at Dallas, Richardson, TX, 75083-0688, USA

ARTICLE INFO

Handling Editor: M. Santosh

ABSTRACT

Collision between the Indian and Eurasian plates formed the ~2500 km long Yarlung Zangbo Suture Zone and produced the Himalaya mountains and Tibetan plateau. Here we offer a new explanation for tectonic events leading to this collision: that the northward flight of India was caused by an Early Cretaceous episode of subduction initiation on the southern margin of Tibet. Compiled data for ophiolites along the Yarlung Zangbo Suture Zone show restricted ages between 120 Ma and 130 Ma, and their supra-subduction zone affinities are best explained by seafloor spreading in what became the forearc of a north-dipping subduction zone on the southern margin of Tibet. The subsequent evolution of this new subduction zone is revealed by integrating data for arc-related igneous rocks of the Lhasa terrane and Xigaze forearc basin deposits. Strong slab pull from this new subduction zone triggered the rifting of India from East Gondwana in Early Cretaceous time and pulled it northward to collide with Tibet in Early Paleogene time.

1. Introduction

From the early days of continental drift investigations, scientists have wondered why India suddenly rifted away from Eastern Gondwana ~130 million years ago and drifted rapidly north to collide with Asia 75 million years later. Here we use our new understanding of how new subduction zones form to show that creation of a new subduction zone on the southern margin of Tibet was responsible. Because subduction initiation (SI) generally requires >1000 km lithospheric failure resulting in a long region of simultaneous seafloor spreading above the sinking oceanic lithosphere, belts of supra-subduction zone ophiolites formed during SI have become keys for recognizing ancient sites of subduction zone formation (Stern et al., 2012). Such a belt of Early Cretaceous SSZ-type ophiolites is found along the Yarlung Zangbo Suture Zone between the Lhasa terrane (Tibet) and India. In this paper, we integrate existing data for Early Cretaceous rocks of the Lhasa terrane of southern Tibet, including ophiolites, metamorphic soles, arc-related plutons and volcanic rocks, and forearc basin deposits with paleomagnetic data. We use this to document SI for this region and show how this new subduction zone pulled India northward, causing the Himalayan collision that continues today.

2. Data

To document the formation of a new subduction zone on the S. flank of the Lhasa Terrane and show how this led to the northward flight of India from E. Gondwana, six independent lines of evidence are presented below: (A) Formation of Early Cretaceous ophiolites as a result of seafloor spreading above a sinking slab of Neotethys during SI; (B) Formation of metamorphic soles by juxtaposition of hot mantle and cold downgoing sediments during SI; (C) Paleomagnetic results consistent with the formation of these ophiolites along the southern margin of the Lhasa terrane; (D) The Indus-Xigaze forearc basin as a record of arc evolution; (E) Evolution of a magmatic arc to the north of the ophiolite belt and forearc basin; and (F) What we know about the northward drift of India. These items are briefly discussed below. We also briefly comment on the presence of UHP phases in these ophiolitic rocks as well.

2.1. Early Cretaceous ophiolites of the Yarlung Zangbo Suture Zone

Geologic studies since the late 1990's have increasingly targeted ophiolites of the Yarlung Zangbo Suture Zone (YZSZ) (Hébert et al., 2012). These ophiolites form an E–W-trending belt that can be traced for about 2000 km from the central segment of the YZSZ to southern Ladakh

* Corresponding author.
E-mail address: rjstern@utdallas.edu (R.J. Stern).
Peer-review under responsibility of China University of Geosciences (Beijing).

https://doi.org/10.1016/j.gsf.2020.01.010
Received 4 December 2019; Received in revised form 15 January 2020; Accepted 26 January 2020
Available online 11 February 2020

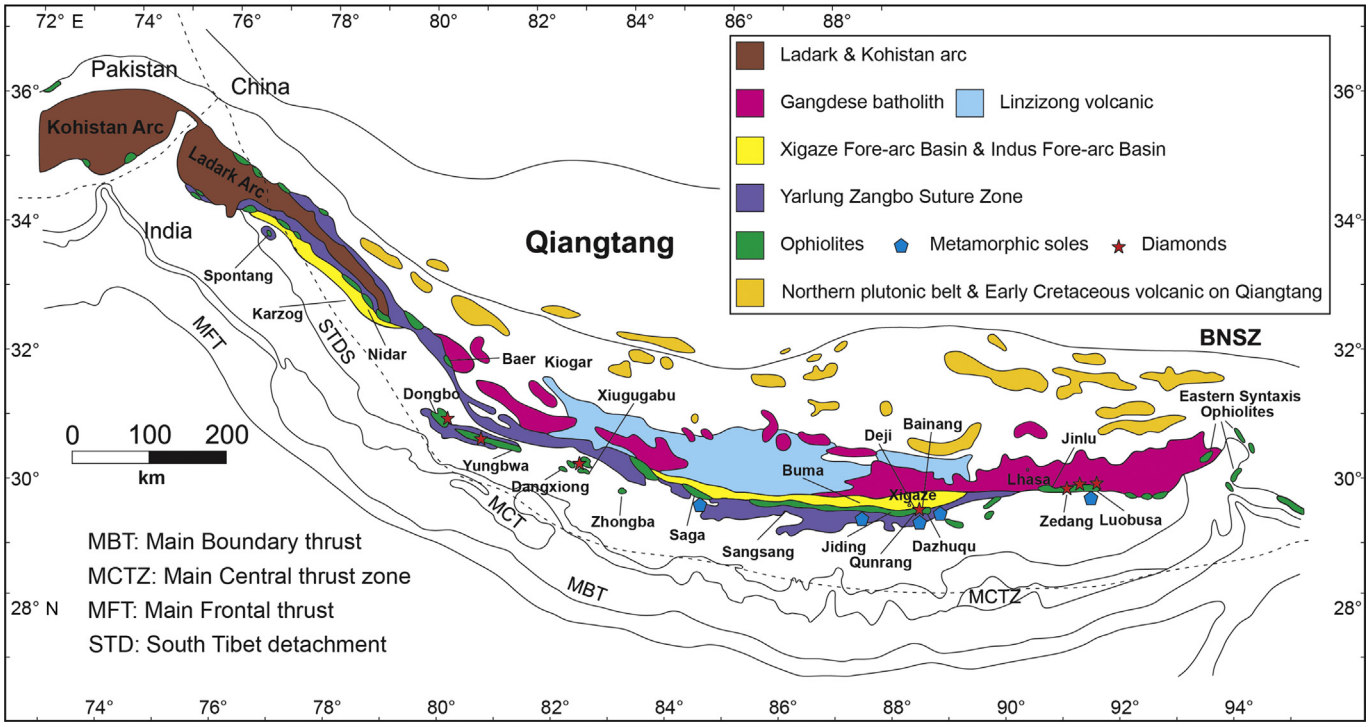

Fig. 1. Simplified tectonic map of southern Tibet showing major ophiolitic massifs of the Yarlung Zangbo Suture Zone, Xigaze and Indus forearc basin and volcanic belts of the Lhasa terrane. Indus forearc basin sources are from An et al. (2014), volcanic sources from Chiu et al. (2009) and Wei et al. (2017). Distributions of plutonic rocks, ophiolitic diamonds and metamorphic soles are also shown. The map is modified after Hébert et al. (2012).

in N. India; correlative Early Cretaceous intra-oceanic arc crust is found in Kohistan in northern Pakistan (Fig. 1). We compiled available geochronologic data for ophiolites from Luobusa in the east to Spontang in the west, including those of the eastern segment (Luobusa, Zedang); central segment (Dazhuqu, Bainang, Deji, Qunrang, Jiding, Buma, Sangsang and Saga); western segment (Zhongba, Xiugugabu, Dangxiong, Yungbwa, Kiogar, Dongbo, Baer) and south Ladakh segment (Nidar, Spontang) (Figs. 2 and 3; Table 1). These ophiolites yield U–Pb zircon ages indicating they mostly formed between 130 Ma and 120 Ma, except for Luobusa, Zedang in the east, and Kiogar, Spontang in the western part

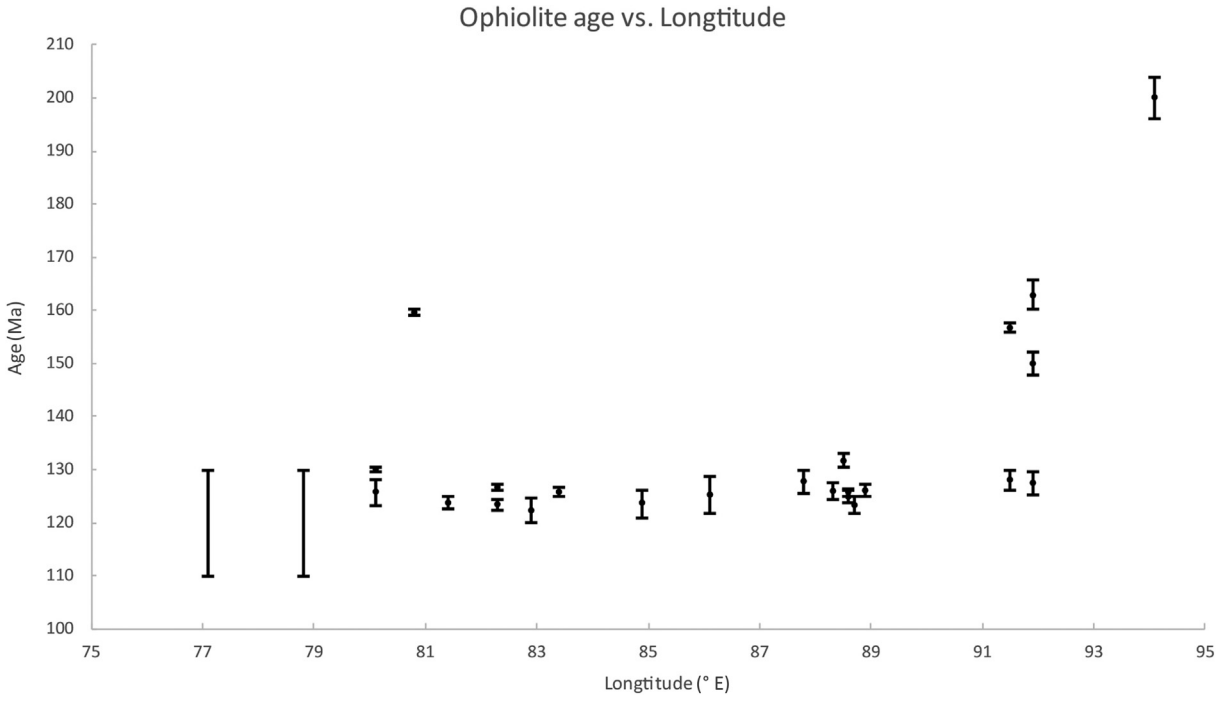

Fig. 2. Plot of ophiolite ages along the Yarlung Zangbo Suture Zone versus longitude, ages listed in Table 1. No systematic variation in age with location along the ophiolite belt is apparent.

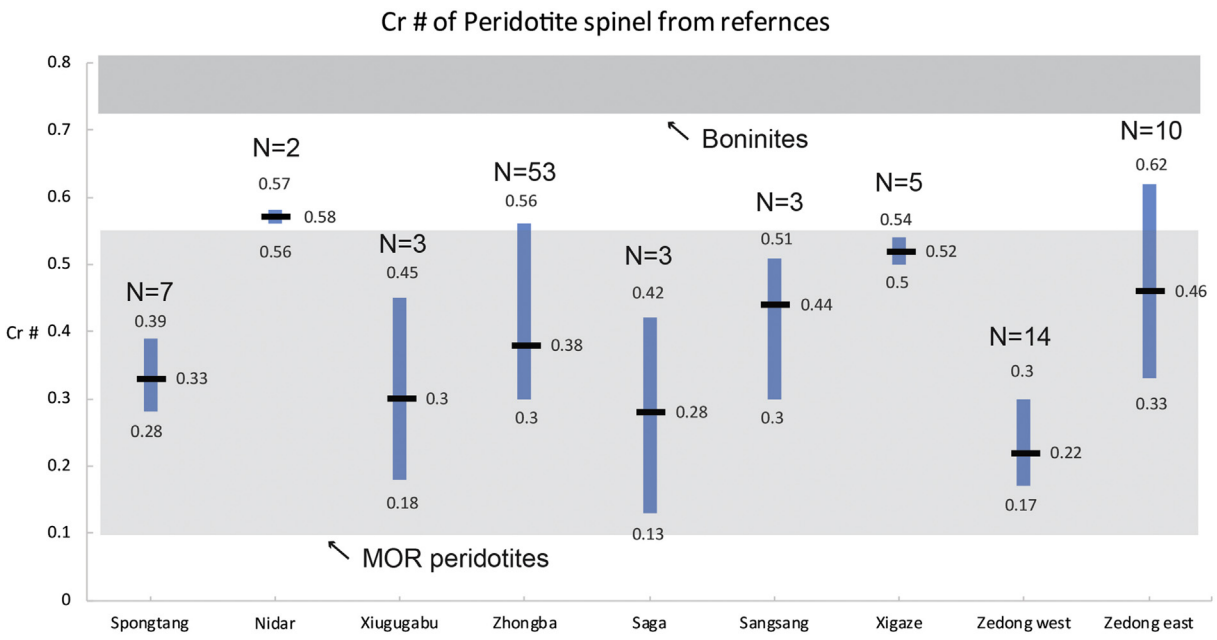

Fig. 3. Cr# [= Cr/(Cr + Al)] for spinels from harzburgite and lherzolite in Zedang (Xiong et al., 2016), Xigaze (Xiong et al., 2017), Sangsang, Saga (Bédard et al., 2009), Zhongba (Dai et al., 2011), Xiugugabu (Bezard et al., 2011), Nidar and Spontang (Mahéo et al., 2004) peridotite massifs. Means of spinel Cr# from each location were calculated from published data in references with sample size (N) indicated on top of each location, and supplementary data listed in Supplementary Table S1. Fields for N-MORB and boninites are taken from (Dick and Bullen, 1984).

of the ophiolite belt, which also contain mid to Late Jurassic ophiolitic remnants (Fig. 4A; Table 1). Dismembered metamorphic soles with similar Early Cretaceous ages are found within ophiolitic melange from the central segment (Guilmette et al., 2009, 2012).

Early Cretaceous YZSZ ophiolites are dismembered (Maffione et al., 2015) but generally include an upper mantle sequence; a few complete Penrose-type ophiolites are preserved in the central and south Ladakh segments. These differ from Late Cretaceous SI ophiolite belt from the eastern Mediterranean to SE Iran and Oman which often show more complete Penrose-type ophiolite sequences (Whattam and Stern, 2011), perhaps because of intense tectonism and erosion associated with India-Tibet collision. Nevertheless, dismembered Early Cretaceous ophiolites of the YZSZ show evidence of upper-plate extension and geochemical fingerprints of arc tholeiitic and boninitic magmatism that are similar to SI ophiolites and to Izu-Bonin-Mariana (IBM) forearc lithosphere (Shervais, 2001; Whattam and Stern, 2011; Maffione et al., 2017). Ophiolitic basalts include N-MORB with small Ta–Nb negative anomalies and more arc-like lavas including boninites, similar to SI sequences documented for the IBM forearc (Reagan et al., 2010). Dai et al. (2013) reported that boninitic dikes in the Xigaze ophiolite gave U–Pb zircon ages of ~125 Ma, and other boninites were also reported from the Xigaze area (Chen et al., 2003; Malpas et al., 2003; Dubois-Côté et al., 2005). Furthermore, Zhong et al. (2019) reported fore-arc basalt-like and boninitic mafic rock in the western YZSZ.

Whattam and Stern (2011) summarized Late Jurassic and Late Cretaceous volcanic sequences in Tethyan ophiolites to establish the 'subduction initiation rule', arguing that most ophiolites form during SI and that the diagnostic magmatic chemostratigraphic progression for such ophiolites is from less to more HFSE-depleted and LILE-enriched compositions. Decompression melting of rising asthenosphere (Fig. 5B) transitions into flux melting as the mantle source is increasingly influenced by slab-derived fluids as SI progresses (Fig. 5C). This is reflected in the evolution from early MORB-like to later arc-like (volcanic arc basalts ± boninites) as SI transitions into true subduction. Consequently, MORB-like and arc-like ophiolite components are expected for SI ophiolites. Cr# [= Cr/(Cr + AL)] of spinels in YZSZ peridotites varies from moderate (0.4–0.6) to high (>0.8) (Fig. 3), as expected for forearc peridotites associated with SI (Stern et al., 2012). Early Cretaceous YZSZ ophiolites likely formed during a SI event lasting 5–10 million years before the convergent margin matured into a N-dipping subduction zone beneath the southern margin of the Lhasa Terrane (Fig. 5C).

2.2. Metamorphic soles

Metamorphic soles at the base of ophiolites are produced when supracrustal rocks are juxtaposed with hot mantle during subduction initiation (van Hinsbergen, 2015). Ophiolite metamorphic soles are thus key indicators of SI and their radiometric ages constrain when this occurred.

Highly foliated garnet-clinopyroxene-amphibolite blocks are documented from the Saga and Xigaze ophiolites (Fig. 1) within serpentinite mélange. This mélange is interpreted as a part of the forearc accretionary complex (Cai et al., 2012). Garnet-amphibolites are interpreted to represent dismembered metamorphic soles and have similar $^{40}Ar/^{39}Ar$ ages (123–132 Ma) to that of the ophiolite. These ages are thought to reflect when high-grade metamorphism ended (Guilmette et al., 2008, 2009, 2012). P-T estimates of these amphibolites indicate these were metamorphosed to pressures of 12 kbar and 850 °C in the Early Cretaceous during the inception of a subduction zone (Guilmette et al., 2012). Younger amphibolites are also reported from S. Lhasa block ophiolites. Malpas et al. (2003) reported $^{40}Ar/^{39}Ar$ ages of 80–90 Ma on amphibole and biotite from Luobusa amphibolite (Fig. 1). They interpreted this as when the ophiolite was obducted onto the Indian passive margin before the collision.

2.3. Paleomagnetic constraints

Three paleomagnetic studies have been conducted on sedimentary rocks overlying YZSZ ophiolites. Pozzi et al. (1984) measured about 100 samples from Cheujeon and Xigaze Group sediments near Xigaze, concluding that this ophiolite and its cover formed at 10°–20° N, near where they are today (~30° N). Abrajevitch et al. (2005) measured chert,

Table 1
Synthesis of ages and tectonic setting of the Yarlung Zangbo Ophiolite and Xigaze Fore-arc Basin.

Ophiolites/ Locality	Rock type	Method	Age (Ma)	Reference
Eastern Syntaxis	Ultra mafic	Clinopyroxene ^{40}Ar–^{39}Ar	200 ± 4	Geng et al. (2006)
Luobusa	Gabbroic dyke	Zircon U–Pb	149.9 ± 2.2	Chan et al. (2015)
	Amphibolite (metamorphic sole)	Hornblende ^{40}Ar–^{39}Ar	127.4 ± 2.3	Guilmette et al. (2009)
	Gabbro dike	Whole-rock Sm–Nd	177 ± 31	Zhou et al. (2002)
	Diabase	Zircon U–Pb	162.9 ± 2.8	Zhong et al. (2006)
Zedang	Dolerite dyke	Zircon U–Pb	128 ± 2	Xiong et al. (2016)
	Andesite dike, quartz diorite	Hornblende ^{40}Ar–^{39}Ar	156.8 ± 0.8	McDermid et al. (2002)
Dazhuqu	Dolerite dike	Zircon U–Pb	126.1 ± 1.3	Dai et al. (2013)
	Radiolarian fauna	Radiolarian	130–112	Ziabrev et al. (2003)
	Quartz diorite	Zircon U–Pb	126 ± 1.5	Malpas et al. (2003)
Bainang	Amphibolite (metamorphic sole)	Hornblende ^{40}Ar–^{39}Ar	127.4 ± 2.3	Guilmette et al. (2009)
	Amphibolite (metamorphic sole)	Hornblende ^{40}Ar–^{39}Ar	123.6 ± 2.9	Guilmette et al. (2007)
	Quartz diorite dike	Zircon U–Pb	123.3 ± 1.5	Guilmette et al. (2009)
Deji	Dolerite dike	Zircon U–Pb	124.9 ± 1.1	Dai et al. (2013)
	Dolerite sheeted dike	Zircon U–Pb	126.5 ± 4.7	Dai et al. (2013)
Qunrang	Gabbro	Zircon U–Pb	125.6 ± 0.8	Li et al. (2009)
Xigaze	Gabbro	Zircon U–Pb	131.8 ± 1.3	Chan et al. (2015)
Jiding	Gabbro	Zircon U–Pb	126 ± 1.5	Wang et al. (2006)
	Gabbro dike	Zircon U–Pb	127.1 ± 3.5	Dai et al. (2013)
Buma	Amphibolite (metamorphic sole)	Hornblende ^{40}Ar–^{39}Ar	127.7 ± 2.2	Guilmette et al. (2009)
Sangsang	Dolerite	Zircon U–Pb	125.2 ± 3.4	Bédard et al. (2009)
Saga	Amphibolite (metamorphic sole)	Hornblende ^{40}Ar–^{39}Ar	123.5 ± 2.6	Guilmette et al. (2012)
Zhongba	Dolerite	Zircon U–Pb	125.7 ± 0.9	Dai et al. (2012)
	Diabase	Zircon U–Pb	127.2 ± 1.1	Dai et al. (2011)
Xiugugabu	Dolerite	Zircon U–Pb	122.3 ± 2.4	Bezard et al. (2011)
	Micro-gabbro	Zircon U–Pb	122.3 ± 2.4	Wei et al. (2006)
	Micro-gabbro	Bulk rock Sm–Nd	126.2 ± 9.1	Xu et al. (2008)
Dangxiong	Gabbro	Zircon U–Pb	126.7 ± 0.50	Chan et al. (2015)
	Gabbro	Zircon U–Pb	123.4 ± 1.0	Chan et al. (2015)
Yungbwa	Gabbro	Zircon U–Pb	123.8 ± 1.1	Chan et al. (2015)
	Gabbronorite	Zircon U–Pb	123.4 ± 1.1	Chan et al. (2015)
	Tholeiitic dike	Hornblende ^{40}Ar–^{39}Ar	152 ± 33	Miller et al. (2003)
	Gabbro	Zircon U–Pb	123.4 ± 0.9	Chan et al. (2007)
Kiogar	Gabbronorite dike	Zircon U–Pb	159.7 ± 0.5	Chan et al. (2015)
Dongbo	Pyroxenite dike	Zircon U–Pb	130.0 ± 0.5	Xiong et al. (2011)
	Gabbro dike	Zircon U–Pb	128.0 ± 1.1	Xiong et al. (2011)
Baer	Dolerite dike	Zircon U–Pb	125.6 ± 2.4	Zheng et al. (2017)
	Dolerite dike	Zircon U–Pb	126.3 ± 2.4	Zheng et al. (2017)
Nidar	Basaltic andesite	$^{39}Ar/^{40}Ar$ in amphibole	130–110	Mahéo et al. (2004)
	Gabbro	Clinopyroxene, plagioclase and whole rock Sm–Nd	140 ± 32	Ahmad et al. (2008)
Spontang	Diorite	$^{40}Ar/^{39}Ar$ in amphibole	130–110	Mahéo et al. (2004)
	Diorite	K–Ar in hornblende	140–125	Reuber et al. (1989)
	Plagiogranite	Zircon U–Pb	177	Pedersen et al. (2001)
Kohistan Region	Kohistan batholith	Zircon U–Pb	111.52 ± 0.40	Heuberger et al. (2007)
	Jijal Complex	Sm–Nd	118–117	Dhuime et al. (2007)
	Bulk of Kohistan		134–90	Petterson (2010)
	Yasin sediments	Orbitolina fossils	123–99	Pudsey et al. (1986)

Fore-arc Basin	**Main rock types**	**Facies**	**Age (Ma)**	**Reference**
Gyalaze	Foraminiferal wackestone and packstone interbedded with sandstone and conglomerate	Shallow marine		Wang et al. (2012)
Qubeiya	Mudstone, limestone, sandstone	Shallow marine	78–65	Wu et al. (2010)
Padana	Mudstone, siltsone, sandstone, coarse-grained sandstone, with interlayers of limestone	Shallow marine	84–78	Wu et al. (2010)
Ngamring	Upper: Shale, siltstone, with interlayers of sandstone and limestone Middle: Coarse-grained sandstone, with thin layers of limestone Lower: Shale, sandstone, with interlayers and lenses of limestone	Deep sea flysch	107–84	Wu et al. (2010)
Chongdui	Radiolarian-bearing silicalite, coarse-grained sandstone, siltstone, mudstone with limestone in upper part	Pelagic	116–107	Wu et al. (2010)

siliceous mudstones and volcaniclastic rocks from Donglha, Qunrang and Dazhuq, which yielded consistent sub-equatorial paleolatitudes. Abrajevitch et al. (2005) noted that sediments on top of the ophiolite are faulted against the Xigaze Group, suggesting that the Dazhuqu and Xigaze terranes were unrelated before faulting. Huang et al. (2015) measured radiolarites and Xigaze Group turbiditic sandstones unconformably overlying ophiolitic peridotites at Chongdui, Bainang, and Sangsang, obtaining results similar to those of Pozzi et al. (1984). In addition, Chen et al. (2012) carried out a paleomagnetic study of Early Cretaceous volcanic rocks in the central Lhasa terrane, yielding a paleolatitude of 19.8° ± 4.6° N (Fig. 4D). Clearly more paleomagnetic studies are needed to better understand where YZSZ ophiolites formed relative to the Lhasa terrane, but existing paleomagnetic data are consistent with formation along the southern margin of the Lhasa terrane. The northward motion of India is also shown in Fig. 4D.

2.4. Xigaze-Indus forearc basin

Forearc basin successions displaying a shallowing upward trend from pelagic sediments to turbidites to shelfal and fluvial-deltaic sediments are well developed all along the YZSZ in the Indus forearc basin (Ladakh, India) and the Xigaze forearc basin (south Tibet). Depositional and chronostratigraphic relationships show that Xigaze ophiolite is basement to overlying sediments interpreted as forming in a late Early Cretaceous to Early Paleogene forearc basin (Wang et al., 2017), further supporting the interpretation of YZSZ ophiolites as forming in a forearc during SI. These forearc basin sediments provide a way to reconstruct the arc magmatic history of this convergent margin. The Indus-Xigaze forearc basin lies just north of the ophiolite belt, can be traced ~550 km from Xigaze in the east to Zhongba in the west and is up to ~22 km wide (Wu et al., 2010; Wang et al., 2012). Clastic sediment deposition began with older deep-sea fan flysch of the Xigaze Group (Ngamring and Chongdoi formations) followed by shallow marine terrigenous and carbonate rocks of the Cuojiangding Group (Padana, Qubeiya, Quxia, and Gyalaze formations). Xigaze and Cuojiangding Groups filled the Xigaze forearc basin in Albian to Ypresian time. Volcaniclastic sedimentation of the Ngamring Formation began with thick turbiditic sandstones and interbedded shales in late Albian time and transitioned upwards into shelfal, deltaic, and fluvial strata of the Padana Formation in Santonian time as the forearc basin filled (Wu et al., 2010; Wang et al., 2012). Wang et al. (2012) suggested that Xigaze forearc basin clastic sediments were derived from older Jurassic–Early Cretaceous arc-volcanic sedimentary rocks (Yeba Formation and Sangri Group) south of the Gangdese arc based on provenance analysis; they noted that sediment transport was along the forearc basin axis during its early and late stages and across it during its middle stage. Zircon $\varepsilon_{Hf}(t)$ values of tuffs from the Chongdoi Formation suggest two distinct magmatic sources: (1) large positive $\varepsilon_{Hf}(t)$ values (+12 to +17), and (2) negative to slightly positive $\varepsilon_{Hf}(t)$ values (−4.5 to +1), both interpreted as derived from the eroded Cretaceous volcanic rocks in the Gangdese arc (Wu et al., 2010; Dai et al., 2015). An et al. (2014) concluded that there was limited unroofing of the Gangdese arc prior to collision because Ngamring sandstones do not show the expected trend from feldspathic volcaniclastic to quartzo-feldspathic plutoniclastic compositions with time.

2.5. Lhasa Terrane arc igneous rocks

The Transhimalayan batholith crops out north of the Yarlung-Zangpo suture, can be traced WNW-ESE for ~2500 km across the Lhasa terrane, and has long been recognized as the product of Neotethys subduction. These granitoids can be divided into two suites: (1) in the south, the Gangdese Batholith, consisting of Late Cretaceous to Eocene I-type granitoids, and (2) in the north, an Early Cretaceous plutonic belt (Chiu et al., 2009). Gangdese batholith rocks are mostly younger than India-Tibet collision (Fig. 4C) and these magmas were likely related to collision, not subduction (Fig. 4C). Igneous rocks older than ~55 Ma are related to subduction and these mostly lie north of the ophiolite belt and

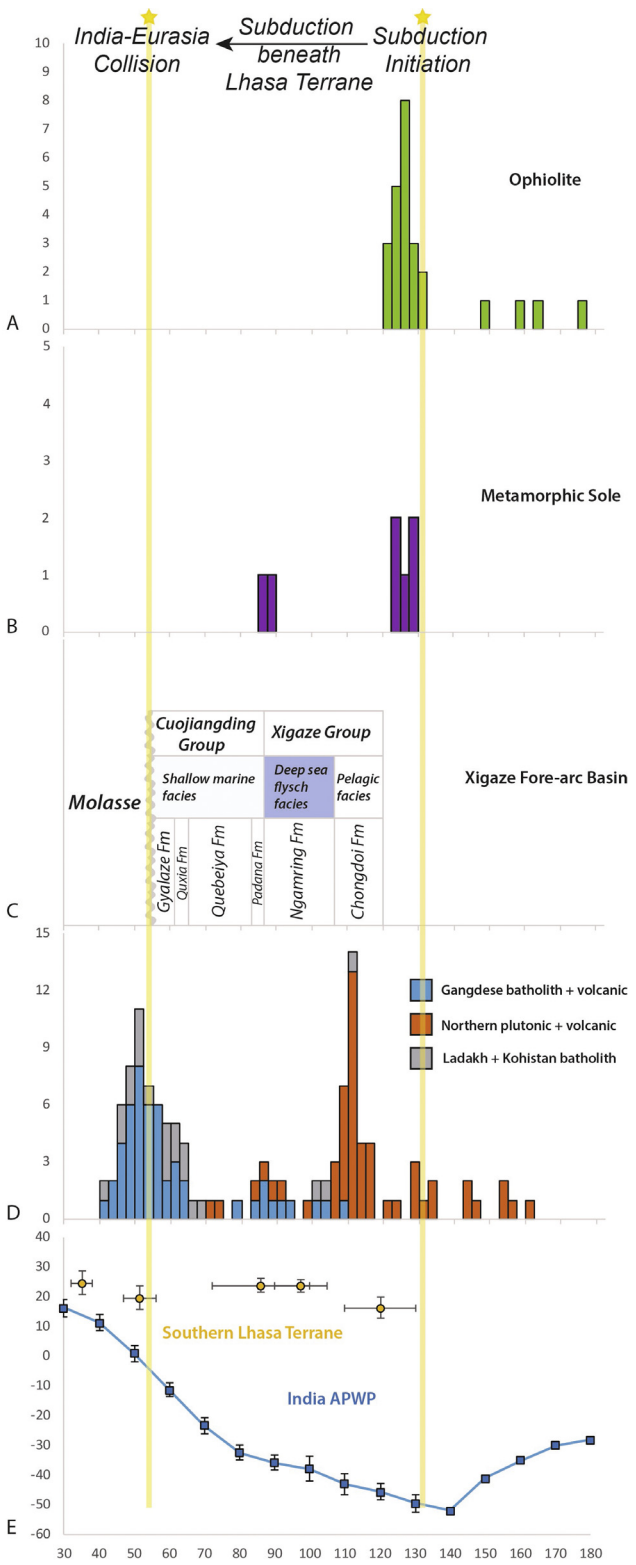

Fig. 4. (A) Histogram of compiled age data for ophiolites along the Yarlung Zangbo Suture Zone, data sources listed in Table 1. (B) Histogram of compiled age data for metamorphic soles within the melange, data sources from Malpas et al. (2003) and Guilmette et al. (2012). (C) Stratigraphic framework of Xigaze forearc basin, modified after Wang et al. (2012). (D) Histogram of compiled age data of plutonic and associated volcanic rocks in the Lhasa terrane, data sources listed in Supplementary Table S2. (E) Paleolatitudes of a reference site (29°N, 88°E) located on the present-day position of the Indus Yarlung Suture Zone, data sources listed in Supplementary Table S3. Northward paleolatitude of India is also shown. See text for further discussion.

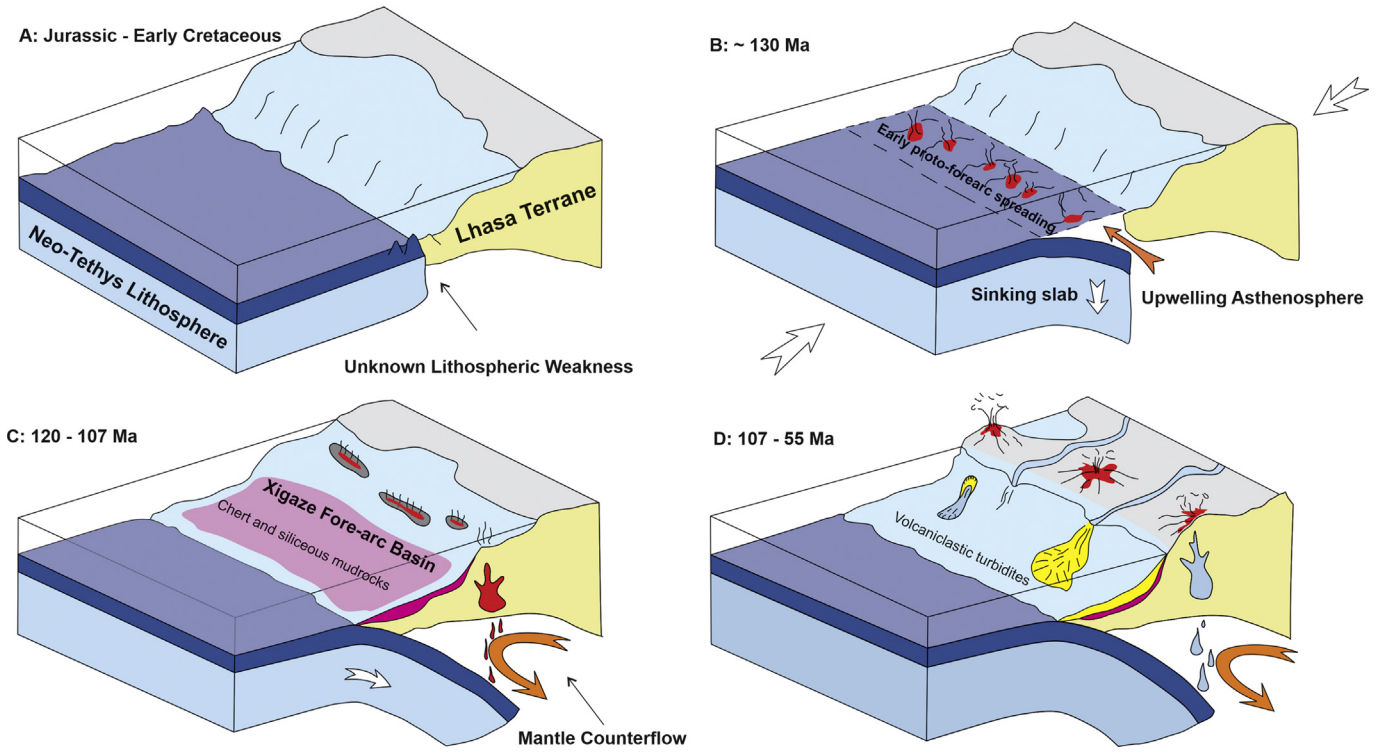

Fig. 5. Schematic reconstructions of the Southern Lhasa Terrane margin from Early Cretaceous to Paleocene time (modified after subduction initiation figure in Whattam and Stern (2011); and Xigaze forearc basin figure in Wang et al. (2017)). (A) Jurassic to Early Cretaceous, a lithospheric weakness is present on the southern margin of the Lhasa terrane, but no convergence between Neo-Tethys and Lhasa terrane during this period; (B) ca. 130 Ma subduction initiation on the southern margin of the Lhasa terrane, decompression melting of upwelling asthenosphere generates ophiolitic magmas that follow the subduction initiation rule (Whattam and Stern, 2011); (C) 120–107 Ma, true subduction begins, with reversal of mantle flow and slow deposition of pelagic sediments in the Xigaze Forearc Basin; (D) 107–55 Ma, main depositional stage of the Xigaze Forearc Basin, which fills with volcaniclastic turbidites eroded from the growing arc to the north. This episode ends when India collides with Eurasia. See text for further discussion.

forearc basin, about where a magmatic arc above a N-dipping subduction zone would be expected; these are the rocks of interest here. Zhu et al. (2009) investigated the genesis of Early Cretaceous igneous rocks of the central Lhasa Terrane, identifying a long magmatic episode (~143–102 Ma) with a flare-up around 110 Ma. Early Cretaceous silicic rocks in the central Lhasa subterrane are metaluminous to peraluminous, enriched in Rb, Th, and U, and depleted in Ba, Nb, Ta, Sr, P, and Ti. These rocks have variably high initial $^{87}Sr/^{86}Sr$ (0.7073–0.7209), negative $\varepsilon_{Nd}(t)$ (−13.7 to −4.6), and negative to positive $\varepsilon_{Hf}(t)$. These signatures indicate an increased mantle component in the generation of the Early Cretaceous melts in the central Lhasa subterrane at ~110 Ma.

Two episodes of volcanism in the Lhasa terrane mirror the Cretaceous-Paleogene intrusive record. These include (1) a more widespread Cretaceous episode (ca. 120–65 Ma) occurring in both the northern and southern magmatic belts, and (2) an intense Paleogene episode (ca. 64–43 Ma) that only took place only in the south. The southward migration and intensification of Lhasa terrane volcanism at ca. 50 Ma is related to collision with India. Prior to collision, widespread Cretaceous volcanism reflected northward subduction underneath the southern margin of the Lhasa terrane.

2.6. Northward drift of India and subduction of Neotethys

Breakup of the Gondwana supercontinent began in the Early Jurassic, with first rifting between S America-Africa-India (W. Gondwana) and Antarctica-Australia (E. Gondwana; Jokat et al., 2003). This was followed by the Cretaceous breakup of eastern Gondwana, resulting in the northward drift of India and culminating in the India-Asia collision. Subduction of Neotethys beneath Tibet was central to these events. Seafloor spreading started northwest of Australia around 136 Ma and propagated SW, reaching the southern tip of India at around 126 Ma (Gibbons et al., 2013). The apparent polar wander path for India suggests that northward drift started around 140 Ma to 130 Ma (Fig. 4D; van Hinsbergen et al., 2012). Separation of India from Madagascar took place in Late Cretaceous time, at 85 Ma to 90 Ma (Gibbons et al., 2013).

2.7. Ultra-high pressure phases

Diamond, coesite and other ultrahigh-pressure minerals have been found in podiform chromitites hosted in several ophiolitic peridotites, such as Kangjinla, Luobusa, Zedang, Xigaze, Dangqiong, Purang and Dongbo (Bai et al., 1993; Yang et al., 2007, 2011; Griffin et al., 2016; Xiong et al., 2016). Unlike diamonds associated with kimberlites, diamonds in these ophiolites are small, mostly from 100 to 200 μm in size. These highly reduced UHP minerals are interpreted to have formed at pressures >4 GPa, corresponding to depths >130 km. It is unclear how these high-P phases became incorporated in the SI ophiolites. Some workers argue that these were transported by plumes (Yang and Dilek, 2015) or otherwise rose from the mantle transition zone (Xiong et al., 2016). Further work is needed to better understand the relationship between UHP phases and Early Cretaceous SI in southern Tibet.

3. Discussion

There are igneous rocks in the southern Lhasa terrane that formed prior to Early Cretaceous subduction initiation. These include Early to Middle Jurassic volcanic rocks of the Bima Formation and Yeba Formation within the Gangdese arc. Because of this, some researchers suggested

that northward subduction underneath the southern margin of the Lhasa terrane might have begun in the Early Jurassic or Late Triassic (Guo et al., 2013; Kang et al., 2014; Kapp and DeCelles, 2019). There are also Late Jurassic Zedong ophiolite and arc remnants in the eastern Yarlung Zangbo Suture Zone, and an ophiolite of similar age has also been found in the western segment at Kiogar, although during this time the Gangdese arc experienced a lull in magmatic activity. These assemblages indicate that tectonic and magmatic activity occurred on the southern margin of the Lhasa terrane prior to Early Cretaceous SI. However, the scattered nature of pre-Early Cretaceous igneous rocks is not consistent with the existence of a robust convergent margin. We do not address whether or not subduction occurred beneath S. Tibet before Cretaceous time, only the strong evidence that a new, north-dipping subduction zone formed here in Early Cretaceous time.

We conclude that no subduction occurred beneath the southern margin of the Lhasa terrane for a significant time prior to lithospheric collapse about 130 Ma. The continent-ocean transition may have been a passive continental margin that likely contained a lithospheric weakness needed to nucleate a new subduction zone (Fig. 5A; Stern and Gerya, 2018). This weakness may have been associated with Jurassic igneous rocks and ophiolites scattered along the southern Lhasa terrane margin (Figs. 1 and 4A). This weakness may have allowed a new subduction zone to form following the final assembly of Tibet in Late Jurassic to Early Cretaceous time when the Lhasa terrane accreted to the Qiangtang terrane, forming the Banggong-Nujiang Suture (Li et al., 2019). Lhasa-Qingtang collision occurred shortly before south Lhasa SI and might have allowed strain to accumulate south of the Lhasa terrane, leading to SI.

Whatever the cause, by 128 Ma Neotethys oceanic lithosphere had sunk sufficiently to allow asthenosphere to flow over it, leading to sea-floor spreading above the sinking slab (Fig. 5B). SI spreading continued for 5–10 million years until the sinking slab started to move down-dip and true subduction began (Fig. 5C). After this time, a normal convergent margin developed and a magmatic arc formed farther north, resulting in widespread Cretaceous igneous activity in the northern and southern magmatic belt (Fig. 5D).

Sedimentary rocks of the Indus-Xigaze fore-arc basin record the evolution of the S. Lhasa terrane convergent margin. After an early stage of slow deposition of pelagic sediment (ca. 120−107 Ma), the fore-arc basin started to fill with volcaniclastic turbidites eroded from the growing arc to the north. As arc volcanoes grew above sealevel, they shed more and more detritus into the forearc basin. This basin gradually evolved from accumulating pelagic sediments to deep sea flysch to shallow marine sediments in Santonian time (83–86 Ma). Eventually the basin became a carbonate platform dominated by limestone interlayered with terrigenous sediments until India collided with Eurasia in Early Paleogene time.

Also during Early Cretaceous time, the northward motion of India began. This is readily explained as a result of slab pull by sinking Neotethys oceanic lithosphere. India's northward motion from Early Cretaceous time until collision was unusually rapid, requiring strong slab pull from a subduction zone (Forsyth and Uyeda, 1975; Chatterjee et al., 2013) in association with push from the Kerguelen plume (Storey, 1995). Kerguelen plume thinned the lithospheric root of the supercontinent (Kumar et al., 2007), which allowed slab pull together with push force provided by plume head to start thr northward drift of India. This unusually rapid northward motion has been explained by multiple mechanisms, including plume head arrival (van Hinsbergen et al., 2011), spontaneous development of cold mantle downwellings inducing mantle drag force underneath India (Yoshida and Hamano, 2015; Yoshida and Santosh, 2018), and two parallel northward-dipping subducting slabs (Jagoutz et al., 2015). The beginning of India's northward flight coincides with Early Cretaceous subduction initiation along the southern Lhasa terrane margin, and this newly formed subduction system could have provided the slab pull needed to separate India from plume-weakened eastern Gondwana and start the northward motion of India.

In brief, taking into account the evidence considered in previous sections, we think that it is useful to apply the subduction initiation model to explain the Early Cretaceous evolution of the southern margin of the Lhasa terrane and the rapid northward flight of India.

4. Conclusion

(1) Andean-type subduction zone initiated along southern margin of Lhasa terrane around 130 Ma, and fore-arc ophiolites and metamorphic soles were generated during the subduction initiation event.
(2) Neotethys seafloor subducted underneath the southern Lhasa terrane until the final collision between India and Eurasia occurred in Paleogene time. A fore-arc basin was progressively filled by sediment sourced from the growing magmatic arc.
(3) Formation of this new subduction zone provided the force needed to separate India from plume-weakened eastern Gondwana and pull it north to collide with Tibet.

Declaration of competing interest

The authors declare that they have no known competing financial interests or personal relationships that could have appeared to influence the work reported in this paper.

Acknowledgments

We appreciate constructive comments and criticisms from Scott A. Whattam, and two anonymous reviewers. We also thank Douwe van Hinsbergen, Carl Guimette and one anonymous reviewer for their comments on a previous version. This is UTD Geosciences contribution number 1358.

Appendix A. Supplementary data

Supplementary data to this article can be found online at https://doi.org/10.1016/j.gsf.2020.01.010.

References

Abrajevitch, A., Aitchison, J.C., Ali, J.R., Badengzhu, Davis, A.M., Liu, J.B., Ziabrev, S.V., 2005. Neotethys and the India–Eurasia collision: insights from a palaeomagnetic study of the Dazhuqu ophiolite southern Tibet. Earth Planet Sci. Lett. 233, 87–102.
Ahmad, T., Tanaka, T., Sachan, H.K., Asahara, Y., Islam, R., Khanna, P.P., 2008. Geochemical and isotopic constraints on the age and origin of the Nidar ophiolitic complex, Ladakh, India: implications for the Neo-Tethyan subduction along the Indus suture zone. Tectonophysics 451, 206–224.
An, W., Hu, X., Garzanti, E., BouDagher-Fadel, M.K., Wang, J., Sun, G., 2014. Xigaze Forearc Basin revisited (South Tibet): provenance changes and origin of the Xigaze ophiolite. Geol. Soc. Am. Bull. 126, 1595–1613.
Bai, W.J., Zhou, M.F., Robinson, P.T., 1993. Possible diamond-bearing mantle peridotites and chromitites in the Luobusa and Donqiao ophiolites, Tibet. Can. J. Earth Sci. 30, 1650–1659.
Bédard, É., Hébert, R., Guilmette, C., Lesage, G., Wang, C.S., Dostal, J., 2009. Petrology and geochemistry of the Saga and Sangsang ophiolitic massifs, Yarlung Zangbo Suture zone, Southern Tibet: evidence for an arc–back-arc origin. Lithos 113, 48–67.
Bezard, R., Hébert, R., Wang, C.S., Dostal, J., Dai, J.G., 2011. Petrology and geochemistry of the Xiugugabu ophiolitic massif western Yarlung Zangbo suture zone, Tibet. Lithos 125, 347–367.
Cai, F., Ding, L., Leary, R.J., Wang, H., Xu, Q., Zhang, L., Yue, Y., 2012. Tectonostratigraphy and provenance of an accretionary complex within the Yarlung–Zangpo suture zone, southern Tibet: insights into subduction–accretion processes in the Neo-Tethys. Tectonophysics 574–575, 181–192.
Chan, G.H.N., Aitchison, J.C., Crowley, Q.G., Horstwood, M.S.A., Searle, M.P., Parrish, R.R., Chan, J.S.L., 2015. U–Pb zircon ages for Yarlung Tsangpo suture zone ophiolites, southwestern Tibet and their tectonic implications. Gondwana Res. 27, 719–732. https://doi.org/10.1016/j.gr.2013.06.016.
Chan, G.H.N., Crowley, Q., Searle, M., Aitchison, J.C., Horstwood, M., 2007. U–Pb Zircon Ages of the Yarlung Zangbo Suture Zone Ophiolites, South Tibet. Abstract Volume 22th Himalaya-Karakoram-Tibet Workshop, p. 12. Hong Kong, China.
Chatterjee, S., Goswami, A., Scotese, C.R., 2013. The longest voyage: tectonic, magmatic, and paleoclimatic evolution of the Indian plate during its northward flight from Gondwana to Asia. Gondwana Res. 23, 238–267.

Chen, G.W., Xia, B., Zhong, Z.H., Wang, G.Q., Wang, H., Zhao, T.P., Wang, J.C., Qi, L., Li, S.R., 2003. Geochemical characteristics and geological significance of boninites in the Deji ophiolite, Tibet. Acta Mineral. Sin. 23, 91–96 (in Chinese with English abstract).

Chen, W., Yang, T., Zhang, S., Yang, Z., Li, H., Wu, H., Zhang, J., Ma, Y., Cai, F., 2012. Paleomagnetic results from the early Cretaceous Zenong group volcanic rocks, Cuoqin, Tibet, and their paleogeographic implications. Gondwana Res. 22 (2), 461–469.

Chiu, H.Y., Chung, S.L., Wu, F.Y., Liu, D.Y., Liang, Y.H., Lin, Y.J., Iizuka, Y., Xie, L.W., Wang, Y.B., Chu, M.F., 2009. Zircon U–Pb and Hf isotope constraints from eastern Transhimalayan batholiths on the precollisional magmatic and tectonic evolution in southern Tibet. Tectonophysics 477, 3–19.

Dai, J.G., Wang, C.S., Hébert, R., Santosh, M., Li, Y.L., Xu, J.Y., 2011. Petrology and geochemistry of peridotites in the Zhongba ophiolite, Yarlung Zangbo Suture zone: implications for the early Cretaceous intra-oceanic subduction zone within the Neo-Tethys. Chem. Geol. 288, 133–148.

Dai, J., Wang, C., Li, Y., 2012. Relicts of the early Cretaceous seamounts in the central-western Yarlung Zangbo Suture zone, southern Tibet. J. Asian Earth Sci. 53, 25–37.

Dai, J.G., Wang, C.S., Polat, A., Santosh, M., Li, Y.L., Ge, Y.K., 2013. Rapid forearc spreading between 130 and 120Ma: evidence from geochronology and geochemistry of the Xigaze ophiolite, southern Tibet. Lithos 172–173, 1–16. https://doi.org/10.1016/j.lithos.2013.03.011.

Dai, J.G., Wang, C.S., Zhu, D.C., Li, Y.L., Zhong, H.T., Ge, Y.K., 2015. Multi-stage volcanic activities and geodynamic evolution of the Lhasa terrane during the Cretaceous: insights from the Xigaze forearc basin. Lithos 218–219, 127–140.

Dhuime, B., Bosch, D., Bodinier, J.L., Garrido, C.J., Bruguier, O., Hussain, S.S., Dawood, H., 2007. Multistage evolution of the Jijal ultramafic–mafic complex (Kohistan, N Pakistan): implications for building the roots of island arcs. Earth Planet Sci. Lett. 261, 179–200.

Dick, H.J.B., Bullen, T., 1984. Chromian spinel as a petrogenetic indicator in abyssal and Alpine-type peridotites and spatially associated lavas. Contrib. Mineral. Petrol. 86 (1), 54–76. https://doi.org/10.1007/BF00373711.

Dubois-Côté, V., Hébert, R., Dupuis, C., Wang, C.S., Li, Y.L., Dostal, J., 2005. Petrological and geochemical evidence for the origin of the Yarlung Zangbo ophiolites, southern Tibet. Chem. Geol. 214, 265–286. https://doi.org/10.1016/j.chemgeo.2004.10.004.

Forsyth, D., Uyeda, S., 1975. On the relative importance of the driving forces of plate motion. Geophys. J. Int. 43, 163–200.

Geng, Q., Pan, G., Zheng, L., Chen, Z., Fisher, R.D., Sun, Z., Ou, C., Dong, H., Wang, X., Li, S., Lou, X., Fu, H., 2006. The Eastern Himalayan syntaxis: major tectonic domains, ophiolitic mélanges and geologic evolution. J. Asian Earth Sci. 27 (3), 265–285. https://doi.org/10.1016/j.jseaes.2005.03.009.

Gibbons, A.D., Whittaker, J.M., Müller, R.D., 2013. The breakup of East Gondwana: assimilating constraints from Cretaceous ocean basins around India into a best-fit tectonic model. J. Geophys. Res. Solid Earth 118, 808–822.

Guilmette, C., Hébert, R., Bédard, É., Wang, C.S., Ullrich, T.D., Dostal, J., 2007. Saga Ophiolite, Yarlung Zangbo Suture Zone, Tibet: Field Relationships, Discovery of Garnet-Pyroxene Amphibolite and Ar/Ar Ages, p. 37. Workshop Abstract Volume, HKTW 22 Hong Kong.

Guilmette, C., Hébert, R., Dupuis, C., Wang, C.S., Li, Z.J., 2008. Metamorphic history and geodynamic significance of high-grade metabasites from the ophiolitic mélange beneath the Yarlung Zangbo ophiolites, Xigaze area, Tibet. J. Asian Earth Sci. 32, 423–437.

Guilmette, C., Hébert, R., Wang, C., Villeneuve, M., 2009. Geochemistry and geochronology of the metamorphic sole underlying the Xigaze ophiolite, Yarlung Zangbo Suture zone, South Tibet. Lithos 112, 149–162.

Guilmette, C., Hebert, R., Dostal, J., Indares, A., Ullrich, T., Bedard, E., Wang, C.S., 2012. Discovery of a dismembered metamorphic sole in the Saga ophiolitic melange, South Tibet: assessing an Early Cretaceous disruption of the Neo-Tethyan supra-subduction zone and consequences on basin closing. Gondwana Res. 22, 398–414.

Guo, L., Liu, Y., Liu, S., Cawood, P.A., Wang, Z., Liu, H., 2013. Petrogenesis of early to middle Jurassic granitoid rocks from the Gangdese belt, Southern Tibet: implications for early history of the Neo-Tethys. Lithos 179, 320–333.

Griffin, W.L., Afonso, J.C., Belousova, E.A., Gain, S.E., Gong, X.H., González-Jiménez, J.M., Howell, D., Huang, J.X., McGowan, N., Pearson, N.J., Satsukawa, T., Shi, R., Williams, P., Xiong, Q., Yang, J.S., Zhang, M., O'Reilly, S.Y., 2016. Mantle recycling: transition zone metamorphism of Tibetan ophiolitic peridotites and its tectonic implications. J. Petrol. 57, 655–684. https://doi.org/10.1093/petrology/egw011.

Hébert, R., Bezard, R., Guilmette, C., Dostal, J., Wang, C.S., Liu, Z.F., 2012. The Indus–Yarlung Zangbo ophiolites from Nanga Parbat to Namche Barwa syntaxes, southern Tibet: first synthesis of petrology, geochemistry, and geochronology with incidences on geodynamic reconstructions of Neo-Tethys. Gondwana Res. 22, 377–397.

Heuberger, S., Schaltegger, U., Burg, J.P., Villa, I.M., Frank, M., Dawood, H., Hussain, S., Zanchi, A., 2007. Age and isotopic constraints on magmatism along the Karakoram–Kohistan Suture Zone, NW Pakistan: evidence for subduction and continued convergence after India–Asia collision. Swiss J. Geosci. 100, 85–107.

Huang, W., van Hinsbergen, D.J., Maffione, M., Orme, D.A., Dupont-Nivet, G., Guilmette, C., Ding, L., Guo, Z., Kapp, P., 2015. Lower Cretaceous Xigaze ophiolites formed in the Gangdese forearc: evidence from paleomagnetism, sediment provenance, and stratigraphy. Earth Planet Sci. Lett. 415, 142–153.

Jagoutz, O., Royden, L., Holt, A.F., Becker, T.W., 2015. Anomalously fast convergence of India and Eurasia caused by double subduction. Nat. Geosci. 8, 475–478.

Jokat, W., Boebel, T., König, M., Meyer, U., 2003. Timing and geometry of early Gondwana breakup. J. Geophys. Res. 108B. https://doi.org/10.1029/2002JB001802.

Kang, Z., Xu, J., Wilde, S.A., Feng, Z., Chen, J., Wang, B., Fu, W., Pan, H., 2014. Geochronology and geochemistry of the Sangri group volcanic rocks, southern Lhasa terrane: implications for the early subduction history of the Neo-Tethys and Gangdese magmatic arc. Lithos 200–201, 157–168.

Kapp, P., DeCelles, P.G., 2019. Mesozoic–Cenozoic geological evolution of the Himalayan-Tibetan orogen and working tectonic hypotheses. Am. J. Sci. 319, 159–254.

Kumar, P., Yuan, X., Kumar, M.R., Kind, Rainer, Li, X., Chadha, R.K., 2007. The rapid drift of the Indian plate. Nature 449, 894–897.

Li, J.F., Xia, B., Liu, L.W., Xu, L.F., He, G.S., Wang, H., Zhang, Y.Q., Yang, Z.Q., 2009. SHRIMP U–Pb dating for the Gabbro in Qunrang Ophiolite, Tibet: the geochronology constraint for the development of eastern Tethys basin. Geotect. Metallogenia 33, 294–298.

Li, S., Yin, C., Guilmette, C., Ding, L., Zhang, J., 2019. Birth and demise of the Bangong-Nujiang Tethyan Ocean: a review from the Gerze area of central Tibet. Earth Sci. Rev. 198, 102907.

Maffione, M., van Hinsbergen, D.J., Koornneef, L.M., Guilmette, C., Hodges, K., Borneman, N., Huang, W., Ding, L., Kapp, P., 2015. Forearc hyperextension dismembered the south Tibetan ophiolites. Geology 43, 475–478.

Maffione, M., van Hinsbergen, D.J.J., de Gelder, G.I.N.O., van der Goes, F.C., Morris, A., 2017. Kinematics of late Cretaceous subduction initiation in the Neo-tethys ocean reconstructed from ophiolites of Turkey, Cyprus, and Syria. J. Geophys. Res. 122, 3953–3976.

Mahéo, G., Bertrand, H., Guillot, S., Villa, I.M., Keller, F., Capiez, P., 2004. The south Ladakh ophiolites (NW Himalaya, India): an intra-oceanic tholeiitic origin with implication for the closure of the Neo-Tethys. Chem. Geol. 203, 273–303.

Malpas, J., Zhou, M.-F., Robinson, P.T., Reynolds, P.H., 2003. Geochemical and geochronological constraints on the origin and emplacement of the Yarlung Zangbo ophiolites, Southern Tibet. In: Dilek, Y., Robinson, P.T. (Eds.), Ophiolites in Earth History, vol. 218. Geological Society of London Special Publication, pp. 191–206.

McDermid, I.R.C., Aitchison, J.C., Davis, A.M., Harrison, T.M., Grove, M., 2002. The Zedong terrane: a late Jurassic intra-oceanic magmatic arc within the Yarlung Zangbo suture zone, southeastern Tibet. Chem. Geol. 187, 267–277.

Miller, C., Thöni, M., Framk, W., Schuster, R., Melcher, F., Meisel, T., Zanetti, A., 2003. Geochemistry of tectonomagmatic affinity of the Yungbwa ophiolite, SW Tibet. Lithos 66, 155–172.

Pedersen, R.B., Searle, M.P., Corfield, R.I., 2001. U–Pb zircon ages from the Spontang ophiolite, Ladakh Himalaya. J. Geol. Soc. London 158, 513–520.

Petterson, M.G., 2010. A review of the geology and tectonics of the Kohistan island arc, north Pakistan. In: Kusky, T.M., Zhai, M.-G., Xiao, W. (Eds.), The Evolving Continents: Understanding Processes of Continental Growth. Geological Society, Special Publications, London, pp. 287–327.

Pozzi, J.P., Westphal, M., Girardeau, J., Besse, J., Yao, X.Z., Xian, Y.C., Li, S.X., 1984. Paleomagnetism of the Xigaze ophiolite and flysch (Yarlung Zangbo suture zone, southern Tibet); latitude and direction of spreading. Earth Planet Sci. Lett. 70, 383–394.

Pudsey, C.J., Schroeder, R., Skelton, P.W., 1986. Cretaceous (Aptian–Albian) age for island arc volcanics, Kohistan, N Pakistan. In: Gupta, V.J. (Ed.), Recent Researches in Geology. Palaeontology: Stratigraphy and Structure of Western Himalayas. Geology of Western Himalayas, vol. 3. Hindustan Publishing Company, Delhi, pp. 150–168.

Reagan, M.K., Ishizuka, O., Stern, R.J., Kelley, K.A., Ohara, Y., Blichert-Toft, J., Bloomer, S.H., Cash, J., Fryer, P., Hanan, B.B., Hickey-Vargas, R., Ishii, T., Kimura, J.-I., Peate, D.W., Rowe, M.C., Woods, M., 2010. Fore-arc basalts and subduction initiation in the Izu-Bonin-Mariana system. G-cubed 11, Q03X12. https://doi.org/10.1029/2009GC002871.

Reuber, I., Montigny, R., Thuizat, R., Heitz, A., 1989. K/Ar ages of ophiolites and arc volcanics of the Indus suture zone: clues on the early evolution of Neotethys. Eclogae Geol. Helv. 82, 699–715.

Shervais, J.W., 2001. Birth, death, and resurrection: the life cycle of suprasubduction zone ophiolites. Geochem. Geophys. Geosyst. 2 (1), 1010. https://doi.org/10.1029/2000GC000080.

Stern, R.J., Gerya, T., 2018. Subduction initiation in nature and models: a review. Tectonophysics 746, 173–198.

Stern, R.J., Reagan, M., Ishizuka, O., Ohara, Y., Whattam, S., 2012. To understand subduction initiation, study forearc crust; to understand forearc crust, study ophiolites. Lithosphere 4, 469–483.

Storey, B.C., 1995. The role of the mantle plumes in continental breakup: case histories from Gondwana. Nature 377, 301–308.

van Hinsbergen, D.J.J., Steinberger, B., Doubrovine, P.V., Gassmöller, V., 2011. Acceleration and deceleration of India-Asia convergence since the Cretaceous: roles of mantle plumes and continental collision. J. Geophys. Res. 116, B06101. https://doi.org/10.1029/2010JB008051.

van Hinsbergen, D.J.J., Peters, K., Maffione, M., Spakman, W., Guilmette, C., Thieulot, C., Plümper, O., Gürer, D., Brouwer, F.M., Aldanmaz, E., Kaymakcı, N., 2015. Dynamics of intraoceanic subduction initiation: 2. Suprasubduction zone ophiolite formation and metamorphic sole exhumation in context of absolute plate motions. Geochem. Geophys. Geosyst. 16, 1771–1785. https://doi.org/10.1002/2015GC005745.

van Hinsbergen, D.J.J., Lippert, P.C., Dupont-Nivet, G., McQuarrie, N., Doubrovine, P.V., Spakman, W., Torsvik, T.H., 2012. Greater India basin hypothesis and a two-stage Cenozoic collision between India and Asia. Proc. Natl. Acad. Sci. Unit. States Am. 109 (20), 7659–7664.

Wang, C.S., Li, X.H., Liu, Z.F., Li, Y.L., Jansa, L., Dai, J.G., Wei, Y.S., 2012. Revision of the Cretaceous–Paleogene stratigraphic framework, facies architecture and provenance of the Xigaze forearc basin along the Yarlung Zangbo suture zone. Gondwana Res. 22, 415–433.

Wang, J., Hu, X., Garzanti, E., An, W., Liu, X.-C., 2017. The birth of the Xigaze forearc basin in southern Tibet. Earth Planet Sci. Lett. 465, 38–47.
Wang, R., Xia, B., Zhou, G., Zhang, Y., Yang, Z., Li, W., Wei, D., Zhong, L., Xu, L., 2006. SHRIMP zircon U–Pb dating for gabbro from the Tiding ophiolite in Tibet. Chin. Sci. Bull. 51, 1776–1779.
Wei, S.-G., Tang, J.X., Song, Y., Liu, Z.B., Feng, J., Li, Y.B., 2017. Early Cretaceous bimodal volcanism in the Duolong Cu mining district, western Tibet: record of slab breakoff that triggered ca. 108–113 Ma magmatism in the western Qiangtang terrane. J. Asian Earth Sci. 138, 588–607.
Wei, Z.Q., Xia, B., Zhang, Y.Q., Wang, R., 2006. SHRIMP zircon dating of diabase in the Xiugugabu ophiolite in Tibet and its geological implications. Geotect. Metallogenia 30, 93–97.
Whattam, S.A., Stern, R.J., 2011. The 'subduction initiation rule': a key for linking ophiolites, intra-oceanic forearcs and subduction initiation. Contrib. Mineral. Petrol. 162, 1031–1045.
Wu, F.Y., Ji, W.Q., Liu, C.Z., Chung, S.L., 2010. Detrital zircon U–Pb and Hf isotopic data from the Xigaze fore-arc basin: constraints on Transhimalayan magmatic evolution in southern Tibet. Chem. Geol. 271, 13–25.
Xiong, F.H., Yang, J.S., Liang, F.H., Ba, D.Z., Zhang, J., Xu, X.Z., Li, Y., Liu, Z., 2011. Zircon U–Pb ages of the Dongbo ophiolite in the western Yarlung Zangbo Suture Zone and their geological significance. Acta Petrol. Sin. 27, 3223–3238.
Xiong, F.H., Yang, J.S., Robinson, P.T., Xu, X.Z., Ba, D.Z., Li, Y., Zhang, Z.M., 2016. Diamonds and other exotic minerals recovered from peridotites of the Dangqiong ophiolite, western Yarlung Zangbo Suture zone, Tibet. Acta Geol. Sin. 90, 425–439.
Xiong, F.H., Yang, J.S., Robinson, P.T., Gao, J., Chen, Y.H., Lai, S.M., 2017. Petrology and geochemistry of peridotites and podiform chromitite in the Xigaze ophiolite, Tibet: implications for a suprasubduction zone origin. J. Asian Earth Sci. 146, 56–75.
Xiong, Q., Griffin, W.L., Zheng, J.-P., O'Reilly, S.Y., Pearson, N.J., Xu, B., Belousova, E.A., 2016. Southward trench migration at ~130–120 Ma caused accretion of the Neo-Tethyan forearc lithosphere in Tibetan ophiolites. Earth Planet Sci. Lett. 438, 57–65.
Xu, J.F., Huang, G., Lei, Y., 2008. Sm–Nd ages and Nd–Sr–Pb isotopic signatures of the Xiugugabu ophiolite, southwestern Tibet. Chin. Geol. 35, 429–435.
Yang, G.X., Dilek, Y., 2015. OIB and P-type ophiolites along the Yarlung Zangbo Suture zone (YZSZ), Southern Tibet: poly-phase melt history and mantle sources of the Neotethyan ocean lithosphere. Episodes 38 (4), 250–265. https://doi.org/10.18814/epiiugs/2015/v38i4/82420.
Yang, J.S., Dobrzhinetskaya, L., Bai, W.J., Fang, Q.S., Robinson, P.T., Zhang, J., Green, H.W., 2007. Diamond- and coesite-bearing chromitites from the Luobusa ophiolite, Tibet. Geology 35, 875–878.
Yang, J.S., Xu, X.Z., Li, Y., Li, J.Y., Ba, D.Z., Rong, H., Zhang, Z.M., 2011. Diamonds recovered from peridotite of the Purang ophiolite in the Yarlung-Zangbo suture of Tibet: a proposal for a new type of diamond occurrence. Acta Petrol. Sin. 27, 3171–3178 (in Chinese with English abstract).
Yoshida, M., Hamano, Y., 2015. Pangea breakup and northward drift of the Indian subcontinent reproduced by a numerical model of mantle convection. Sci. Rep. 5, 8407. https://doi.org/10.1038/srep08407.
Yoshida, M., Santosh, M., 2018. Voyage of the Indian subcontinent since Pangea breakup and driving force of supercontinent cycles: insights on dynamics from numerical modeling. Geosci. Front. 9 (5), 1279–1292. https://doi.org/10.1016/j.gsf.2017.09.001, 2018.
Ziabrev, S.V., Aitchison, J.C., Abrajevitch, A., Badenzhu, Davis A.M., Luo, H., 2003. Precise radiolarian age constraints on the timing of ophiolite generation and sedimentation in the Dazhuqu terrane, Yarlung-Tsangpo suture zone, Tibet. J. Soc. London 160, 591–599.
Zheng, H., Huang, Q.-t., Kapsiotis, A., Xia, B., Yin, Z.-x., Zhong, Y., Lu, Y., Shi, X.-l., 2017. Early Cretaceous ophiolites of the Yarlung Zangbo Suture Zone: insights from dolerites and peridotites from the Baer upper mantle suite, SW Tibet (China). Int. Geol. Rev. 59, 1471–1489.
Zhong, Y., Liu, W.L., Tang, G.J., Liu, N.N., Liu, H.F., Zeng, Q.G., Xia, B., 2019. Origin of Mesozoic ophiolitic mélanges in the western Yarlung Zangbo suture zone, SW Tibet. Gondwana Res. 76, 204–223. https://doi.org/10.1016/j.gr.2019.06.008.
Zhong, L.F., Xia, B., Zhang, Y.Q., Wang, R., Wei, D.L., Yang, Z.Q., 2006. SHRIMP age determination of diabase in Luobusa ophiolite southern Xizang (Tibet). Geol. Rev. 52, 224–229 (in Chinese with English abstract).
Zhou, S., Mo, X.X., Mahoney, J.J., Zhang, S.Q., Guo, T.J., Zhao, T.J., 2002. Geochronology and Nd and Pb isotope characteristics of gabbro dikes in the Luobusa ophiolite, Tibet. Chin. Sci. Bull. 47, 143–146.
Zhu, D.C., Mo, X.X., Niu, Y.L., Zhao, Z.D., 2009. Geochemical investigation of Early Cretaceous igneous rocks along an east–west traverse throughout the central Lhasa Terrane, Tibet. Chem. Geol. 268, 298–312.